# Synergetic formation of secondary inorganic and organic aerosol: Effect of $SO_2$ and $NH_3$ on particle formation and growth

**Biwu Chu**[a, b], **Xiao Zhang**[c], **Yongchun Liu**[a, b, d], **Hong He**[a, b, d *], **Yele Sun**[b,e], **Jingkun Jiang**[c], **Junhua Li**[c], **Jiming Hao**[c]

[a] State Key Joint Laboratory of Environment Simulation and Pollution Control, Research Center for Eco-Environmental Sciences, Chinese Academy of Sciences, Beijing 100085, China

[b] Center for Excellence in Regional Atmospheric Environment, Institute of Urban Environment, Chinese Academy of Sciences, Xiamen 361021, China

[c] State Key Joint Laboratory of Environment Simulation and Pollution Control, School of Environment, Tsinghua University, Beijing 100084, China

[d] University of Chinese Academy of Sciences, Beijing 100049, China

[e] State Key Laboratory of Atmospheric Boundary Layer Physics and Atmospheric Chemistry, Institute of Atmospheric Physics, Chinese Academy of Sciences, Beijing 100029, China

*Correspondence to:* Hong He (honghe@rcees.ac.cn)

## Abstract

The effects of $SO_2$ and $NH_3$ on secondary organic aerosol formation have rarely been investigated together, while the interactive effects between inorganic and organic species under highly complex pollution conditions remain uncertain. Here we studied the effects of $SO_2$ and $NH_3$ on secondary aerosol formation in the photooxidation system of toluene/$NO_x$ in the

presence or absence of $Al_2O_3$ seed aerosols in a 2 $m^3$ smog chamber. The presence of $SO_2$ increased new particle formation and particle growth significantly, regardless of whether $NH_3$ was present or not. Sulfate, organic aerosol, nitrate and ammonium were all found to increase linearly with increasing $SO_2$ concentrations. The increases in these four species were more obvious under $NH_3$-rich conditions, and the generation of nitrate, ammonium and organic aerosol increased more significantly than sulfate with respect to $SO_2$ concentration, while sulfate was the most sensitive species under $NH_3$-poor conditions. The synergistic effects between $SO_2$ and $NH_3$ in the heterogeneous process contributed greatly to secondary aerosol formation. Specifically, the generation of $NH_4NO_3$ was found to be highly dependent on the surface area concentration of suspended particles, and increased most significantly with $SO_2$ concentration among the four species under ammonia-rich conditions. Meanwhile, the absorbed $NH_3$ might provide a liquid surface layer for the absorption and subsequent reaction of $SO_2$ and organic products, and therefore, enhance sulfate and secondary organic aerosol (SOA) formation. This effect mainly occurred in the heterogeneous process, and resulted in a significantly higher growth rate of seed aerosols compared to that without $NH_3$. By applying positive matrix factorization (PMF) analysis to the AMS data, two factors were identified for the generated SOA. One factor, assigned to less-oxidized organic aerosol and some oligomers, increased with increasing $SO_2$ under $NH_3$-poor conditions, mainly due to the well-known acid catalytic effect of the acid products on SOA formation in the heterogeneous process. The

other factor, assigned to the highly oxidized organic component and some nitrogen-containing organics (NOC), increased with $SO_2$ under a $NH_3$-rich environment, with NOC (organonitrates and NOC with reduced N) contributing most of the increase.

## Introduction

With the recent rapid economic development and urbanization, the associated emissions from coal combustion, motor vehicle exhaust and various industrial emissions have led to highly complex air pollution in China. Besides the high concentrations of fine particles ($PM_{2.5}$), high concentrations of $NO_x$, $SO_2$, $NH_3$, and volatile organic compounds (VOCs) were observed in haze pollution episodes (Liu et al., 2013; Ye et al., 2011; Zou et al., 2015; Wang et al., 2015a). China has the highest concentration of $SO_2$ in the world due to a large proportion of energy supply from coal combustion (Bauduin et al., 2016). Surface concentrations of $SO_2$ in the range of a few ppb to over 100 ppb have been observed in north China (Sun et al., 2009; Li et al., 2007). The total emission and concentrations of $SO_2$ have decreased in most regions of China in recent years (Lu et al., 2010; Wang et al., 2015b), but high concentrations of $SO_2$ are still frequently observed. For example, the $SO_2$ concentration was as high as 43 ppb in the winter of 2013 in Jinan city (Wang et al., 2015a), while over 100 ppb $SO_2$ was observed in winter haze days during 2012 in Xi'an city (Zhang et al., 2015). High concentrations of precursors have resulted in high concentrations of secondary inorganic and organic species in $PM_{2.5}$ during

haze formation (Yang et al., 2011; Zhao et al., 2013; Dan et al., 2004; Duan et al., 2005; Wang et al., 2012). There has been no systematic measurement of $NH_3$ in China despite its extensive emission and increasing trend (Fu et al., 2015). A few studies have reported high concentrations of $NH_3$ (maximum concentration higher than 100 ppb) in the North China Plain (Meng et al., 2015; Wen et al., 2015) and many observational data indicated $NH_3$-rich conditions for secondary aerosol formation, and strong correlations between peak levels of fine particles and large increases in $NH_3$ concentrations in China (Ye et al., 2011;Liu et al., 2015a). Unlike $SO_2$, the emission of $NH_3$ is mainly from non-point sources, which are difficult to control, and shows an increasing trend in China (Dong, 2010). Under this complex situation, studying the synergistic effects of $SO_2$ and $NH_3$ in secondary aerosol formation is crucial in order to understand the formation mechanism for heavy haze pollution.

Interactions between inorganic pollutants in secondary aerosol formation have been investigated extensively. For example, $NO_2$ was found to increase the oxidation of $SO_2$ in aqueous aerosol suspensions (Tursic and Grgic, 2001) and on a sandstone surface (Bai et al., 2006). Synergistic reaction between $SO_2$ and $NO_2$ on mineral oxides was reported (Liu et al., 2012a) and was proposed to explain the rapid formation of sulfate in heavy haze days (He et al., 2014). The presence of $NH_3$ could also enhance the conversion of $SO_2$ to sulfate in aerosol water and on the surface of mineral dust or $PM_{2.5}$ (Tursic et al., 2004; Behera and Sharma, 2011; Yang et al., 2016).

Secondary aerosol formation from coexisting inorganic and organic pollutants is far more complicated. There have been a few studies that investigated the effects of $SO_2$ or $NH_3$ on secondary organic aerosol (SOA) formation. $SO_2$ has been found to enhance SOA yield from isoprene (Edney et al., 2005; Kleindienst et al., 2006; Lin et al., 2013), $\alpha$-pinene (Kleindienst et al., 2006; Jaoui et al., 2008), and anthropogenic precursors (Santiago et al., 2012). The enhancing effect is mainly due to the fact that the acidic aerosol products of $SO_2$ can either take up organic species (Liggio and Li, 2008, 2006) or increase the formation of high molecular weight compounds in acid-catalytic reactions (Liggio et al., 2007; Kleindienst et al., 2006; Santiago et al., 2012). Besides, sulfate esters can also contribute to SOA formation (Schmitt-Kopplin et al., 2010). The effects of $NH_3$ on SOA formation are relatively poorly understood. In previous studies, disparate effects of $NH_3$ on secondary aerosol formation were reported. $NH_3$ increased SOA formation from ozonolysis of $\alpha$-pinene or cyclohexene (Na et al., 2007), but had little effect on SOA mass from ozonolysis of isoprene (Na et al., 2007; Lin et al., 2013) and even decreased SOA production from ozonolysis of styrene (Na et al., 2006). $NH_3$ was reported to react with some organic acids and contribute to secondary aerosol formation (Na et al., 2007; Lin et al., 2013), while its nucleophilic attack might decompose trioxolane and hydroxyl-substituted esters and decrease SOA mass (Na et al., 2006). Updyke et al. (2012) studied brown carbon formation via reactions of ammonia with SOA from various precursors. It was found that the degree of browning had a positive

120 correlation with the carbonyl products, which may react with $NH_3$ or $NH_4^+$
121 ion and generate hemiaminal (Amarnath et al., 1991).
122 The effects of $SO_2$ and $NH_3$ on SOA formation have rarely been
123 investigated together, while the interactive effects between inorganic and
124 organic species under highly complex pollution conditions remain
125 uncertain. This study investigated secondary aerosol formation in the
126 photooxidation of toluene/$NO_x$ with varied concentrations of $SO_2$ under
127 $NH_3$-poor and $NH_3$-rich conditions. Some synergetic effects in the
128 heterogeneous process that contributed to both secondary inorganic and
129 organic aerosol formation were explored.

130 ## Methods

131 A series of smog chamber experiments were carried out to simulate
132 secondary aerosol formation in the photooxidation of toluene/$NO_x$ in the
133 presence or absence of $SO_2$ and/or $NH_3$. The chamber is a 2 $m^3$ cuboid
134 reactor constructed with 50 $\mu m$-thick FEP-Teflon film (Toray Industries,
135 Inc., Japan). The chamber was described in detail in Wu *et al.* (2007). A
136 temperature-controlled enclosure (SEWT-Z-120, Escpec, Japan) provides
137 a constant temperature (30 ±0.5 ℃), and 40 black lights (GE F40T12/BLB,
138 peak intensity at 365 nm, General Electric Company, USA) provide
139 irradiation during the experiments. The hydrocarbon concentration was
140 measured by a gas chromatograph (GC, Beifen SP-3420, Beifen, China)
141 equipped with a DB-5 column (30 m ×0.53 mm ×1.5 mm, Dikma, USA) and
142 flame ionization detector (FID), while $NO_x$, $SO_2$ and $O_3$ were monitored

143 by an $NO_x$ analyzer (Model 42C, Thermo Environmental Instruments,
144 USA), an $SO_2$ analyzer (Model 43I, Thermo Environmental Instruments,
145 USA) and an $O_3$ analyzer (Model 49C, Thermo Environmental Instruments,
146 USA), respectively. A scanning mobility particle sizer (SMPS) (TSI 3936,
147 TSI Incorporated, USA) was used to measure the size distribution of
148 particulate matter (PM) in the chamber, and also employed to estimate the
149 volume and mass concentration. The chemical composition of aerosols was
150 measured by an aerosol chemical speciation monitor (ACSM, Aerodyne
151 Research Incorporated, USA) or high resolution time of flight aerosol mass
152 spectrometer (HR-ToF-AMS, Aerodyne Research Incorporated, USA).
153 ACSM is a simplified version of aerosol mass spectrometry (AMS), with
154 similar principles and structure. Ng *et al.* (2011) presented a detailed
155 introduction to this instrument and found that the measurement results
156 agreed well with those of AMS. The chamber was run as a batch reactor in
157 this study. Deposition of particles and gas compounds on the wall was
158 considered to be a first-order process. The deposition rates of particles with
159 different sizes (40-700 nm) were measured under dark conditions. Then,
160 wall losses of particles in the chamber was similarly corrected using a
161 regression equation to describe the dependence of deposition rate on the
162 particle size (Takekawa et al., 2003). Detailed information on this equation
163 was given in our previous studies (Chu et al., 2012; Chu et al., 2014). The
164 deposition of gas phase compounds was determined to be 0.0025 $h^{-1}$,
165 0.0109 $h^{-1}$, 0.0023 $h^{-1}$ and 0.006 $h^{-1}$ for $NO_2$, $O_3$, NO and toluene,
166 respectively. In this study, the wall loss of aerosol mass was about 30%-

50% of total secondary aerosol mass, while the deposition of gas phase compounds was less than 5% of their maximum concentrations in the experiments.

Prior to each experiment, the chamber was flushed for about 40 h with purified air at a flow rate of 15 L/min. In the first 20 h, the chamber was exposed to UV light at 34 ℃. In the last several hours of the flush, humid air was introduced to obtain the target RH, which was 50% in this study. After that, alumina seed particles were added into the chamber. Alumina seed particles were produced on-line via a spray pyrolysis setup, which has been described in detail elsewhere (Liu et al., 2010). Liquid alumisol (AlOOH, Lot No. 2205, Kawaken Fine Chemicals Co., Ltd., Japan) with an initial concentration of 1.0 wt% was sprayed into droplets by an atomizer. After that, the droplets were carried through a diffusion dryer and a corundum tube embedded in a tubular furnace with the temperature maintained at 1000 ℃ to generate alumina particles. The obtained alumina particles were γ-$Al_2O_3$ as detected by X-ray diffraction measurements, and spherical-shaped according to electron micrograph results. Before being introduced into the chamber, the particles were carried through a neutralizer (TSI 3087, TSI Incorporated, USA). Then, toluene was injected into a vaporizer and carried into the chamber by purified air, while $NO_x$, $SO_2$ and $NH_3$ were directly injected into the chamber from standard gas bottles using mass flow controllers. Before adding $NH_3$ into the chamber, $NH_3$ gas was passed through the inlet pipeline for about 15 minutes to reduce absorption within the line. The concentrations of $NH_3$ were

191 estimated according to the amount of $NH_3$ introduced and the volume of
192 the reactor. These experiments with $NH_3$ added to the chamber were
193 referred to as $NH_3$-rich experiments in this study, since the concentrations
194 of $NH_3$ were not measured and it was difficult to estimate the uncertainty
195 of the calculated $NH_3$ concentration. The experiments were carried out at
196 30 ℃ with an initial RH of 50%. During the reaction, the temperature was
197 kept nearly constant (30±0.5 ℃) in the temperature-controlled enclosure,
198 while the RH decreased to 45%-47% at the end of the experiment.

## 199 Results and discussion

### 200 Particle formation and growth in different inorganic gas conditions

201 First, the effects of $SO_2$ and $NH_3$ on secondary aerosol formation were
202 qualitatively studied in the photooxidation system of toluene/$NO_x$ without
203 the presence of a seed aerosol. Experiments were carried out in the absence
204 of $SO_2$ and $NH_3$, in the presence of $SO_2$ or $NH_3$, and coexistence of $SO_2$
205 and $NH_3$, respectively. Experimental details are listed in Table 1. The letter
206 codes used for the experiments represent a combination of the initial letters
207 of the precursors for each experiment. For example, experiment "ASTN"
208 is an experiment with presence of ammonia gas (A), sulfur dioxide (S),
209 toluene (T) and nitrogen oxides (N). Two experiments (ATN and ATN2)
210 were carried out under similar conditions to test the reproducibility of the
211 experiments. Time variations of gas phase compounds of these
212 experiments are shown in Fig. S1 in the supporting information. The

213 presence of $SO_2$ and/or $NH_3$ had no obvious effect on the gas phase
214 compounds, including toluene, $NO_x$, $SO_2$ and $O_3$.

215 Secondary aerosol formation in these photooxidation experiments was
216 measured by the SMPS, and the results are displayed in Figure 1.
217 Compared to toluene/$NO_x$ photooxidation, the secondary aerosol volume
218 concentration rose 1.5 times in the presence of $SO_2$, and was more than
219 tripled in the presence of $NH_3$. The volume of secondary aerosol showed
220 an obvious peak in the toluene/$NO_x$/$NH_3$ system at about 2.3 hours of
221 photooxidation. With the wall deposition accounted for, the decrease of the
222 volume concentration after that point was unexpected, but could be
223 reproduced (Experiments ATN and ATN2). Such a decrease was not
224 observed with coexisting $NH_3$ and $SO_2$, indicating interactions between
225 $NH_3$ and $SO_2$ in the photooxidation system. The reason for this
226 phenomenon will be discussed in the following analysis of the chemical
227 composition of the generated particles.

228 Table 1. Initial experimental conditions of toluene/$NO_x$ photooxidation in the
229 presence or absence of $SO_2$ and/or $NH_3$

| **Experiment No.** | **Toluene** *ppm* | **NO** *ppb* | **$NO_x$-NO** *ppb* | **$SO_2$** *ppb* | **$NH_3$*** *ppb* | **RH** *%* | **T** *K* |
|---|---|---|---|---|---|---|---|
| TN | 1.05 | 54 | 49 | 0 | 0 | 50 | 303 |
| STN | 1.05 | 55 | 50 | 137 | 0 | 50 | 303 |
| ATN | 1.06 | 47 | 48 | 0 | 264 | 50 | 303 |
| ATN2 | 0.98 | 48 | 54 | 0 | 264 | 50 | 303 |

| | | | | | | | |
|---|---|---|---|---|---|---|---|
| ASTN | 1.02 | 49 | 53 | 134 | 264 | 50 | 303 |

*The concentrations of $NH_3$ were calculated according to the amount of $NH_3$ introduced and the volume of the reactor.

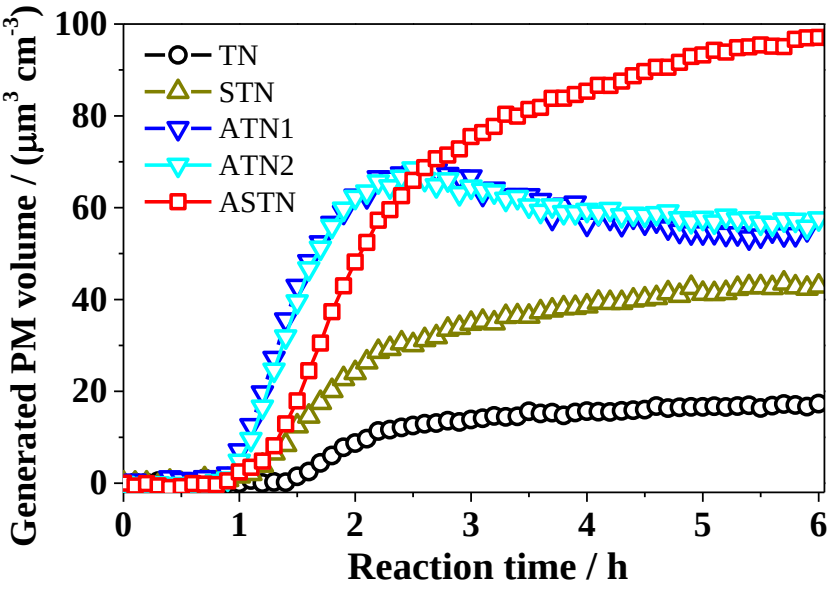


Figure 1. Secondary aerosol formation in photooxidation of toluene/$NO_x$ in the presence or absence of $NH_3$ and/or $SO_2$. The letter codes for the experiments indicate the introduced pollutants, i.e. "A" for ammonia, "S" for sulfur dioxide, "T" for toluene and "N" for nitrogen dioxide. Experimental details are listed in Table 1.

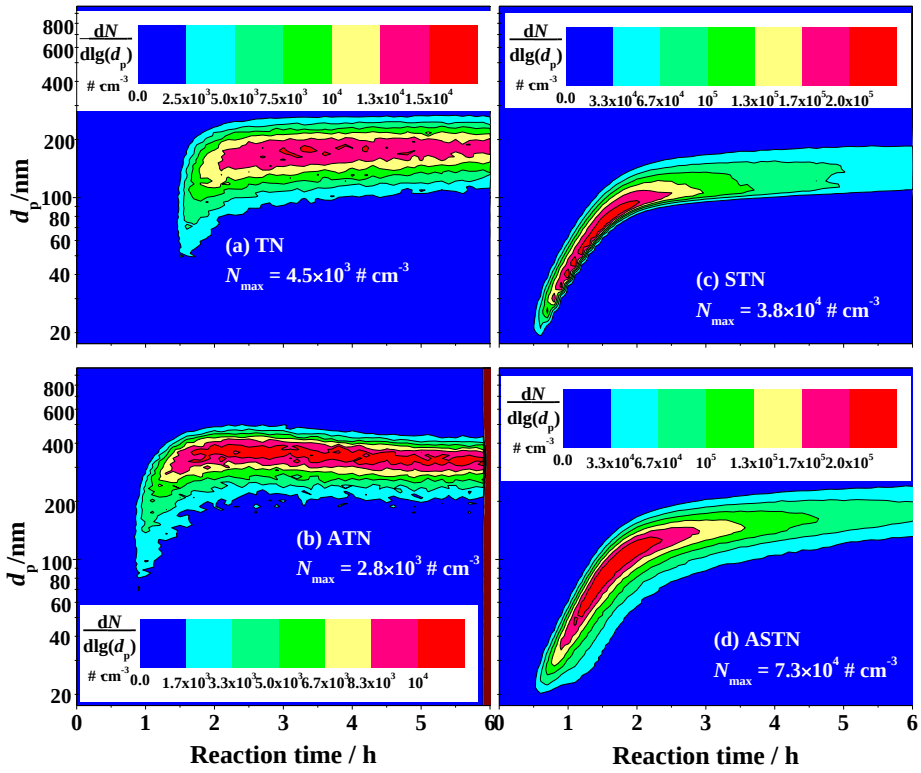


Figure 2. Size distributions of the suspended particles as a function of time during the reaction in photooxidation of toluene/$NO_x$ in the presence or absence of $NH_3$ and/or $SO_2$. $N_{max}$ shows the maximal particle number concentration during the reaction for each experiment. Experimental details are listed in Table 1.

The size distributions of the secondary aerosol in the photooxidation, with a range of 17-1000 nm, were analyzed and are shown in Figure 2. The new particle formation was not directly measured in this study, but the newly generated particles could be detected when the particles increased in size. According to the particle number concentrations, new particle formation appeared to increase a great deal in the presence of $SO_2$. The maximal particle number concentrations in experiments ASTN and STN were one order of magnitude higher than those in experiments ATN and

TN. The presence of $NH_3$ also contributed substantially to the particle growth in photooxidation of toluene/$NO_x$. Comparing Figure 2(c) to Figure 2(a), the total number concentration of particles in experiment ATN was a little lower than that in experiment TN, but the mode diameter of the particles was much larger.

**Secondary inorganic aerosol formation**

Some synergetic effects were observed in secondary inorganic aerosol formation besides the generation of ammonium and sulfate from $NH_3$ and $SO_2$. For example, nitrate formation (which may include both inorganic nitrate and organic nitrates) was not only enhanced by $NH_3$, but also was markedly affected by $SO_2$. The chemical compositions of the aerosols generated in the photooxidation of toluene/$NO_x$ were analyzed with an ACSM, and their time variations are displayed in Figure 3. Since the ACM or AMS cannot distinguish organic salts and organic nitrates, the measured sulfate, nitrate, ammonium were all considered secondary inorganic aerosol, while the organics were all considered secondary organic aerosol in this study. In experiment ATN, the concentrations of ammonium and nitrate decreased after about 2.3 hours of reaction, as shown in Fig. 3, which was consistent with the decreasing trend of particle concentration shown in Fig. 1. The reason for this phenomenon is unknown, but we speculate that the generated $NH_4NO_3$ might partition back into the gas phase as reaction goes on. Detailed simulation results based on the AIM Aerosol Thermodynamics Model (Clegg and Brimblecombe, 2005; Clegg

et al., 1998; Carslaw et al., 1995) are shown in Fig. S3 in the supporting information. The deposition of $NH_3$ in the experiment was likely to shift the partition equilibrium to the gas phase and reduce the concentration of $NH_4NO_3$ salt. In addition, the wall deposition of aerosols might also introduce some error in the concentrations of $NH_4NO_3$ salt, although wall deposition was corrected using an empirical function based on deposition rates of $(NH_4)_2SO_4$ aerosol with different sizes (Chu et al., 2012; Chu et al., 2014). Adding $SO_2$ to the system resulted in a lower peak concentration but a higher final concentration of nitrate. In the presence of $SO_2$, higher concentrations of sulfate and organic species were generated and mixed with nitrate in the aerosol, which may shift the partition balance of $NH_4NO_3$ to the aerosol phase. Some simulation results using the AIM Aerosol Thermodynamics Model with different concentrations of sulfate are also shown in Fig. S3 in the supporting information. In addition, in the presence of organic matter, $(NH_4)_2SO_4$ aerosol might deliquesce at a RH lower than the deliquescence relative humidity (DRH) (Meyer et al., 2009; Li et al., 2014). If this took place in the experiment, sulfate might provide moist surfaces for heterogeneous hydrolysis of $N_2O_5$, contributing to nitrate formation due to the high uptake coefficient of $N_2O_5$ on ammonium sulfate (Pathak et al., 2009;Hallquist et al., 2003;Hu and Abbatt, 1997). $N_2O_5$ was not measured in this study, but it was expected to be generated in the presence of $NO_2$ and $O_3$ in the experiments.

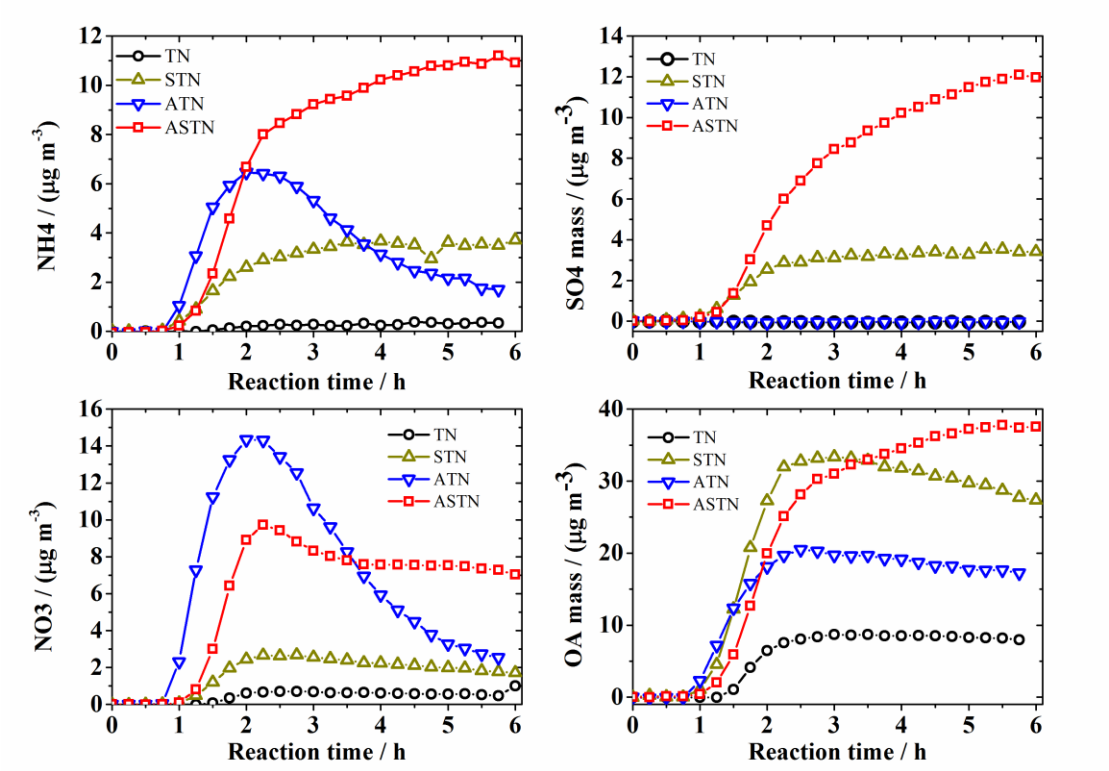


Figure 3. Time variations of the chemical species in the secondary aerosol generated from the photooxidation of toluene/$NO_x$ in the presence or absence of $NH_3$ and $SO_2$. Letter codes for experiments indicate the introduced pollutants, i.e. "A" for ammonia, "S" for sulfur dioxide, "T" for toluene and "N" for nitrogen dioxide. Experimental details are listed in Table 1.

In Figure 3, the generation of ammonium salt can be observed in the photooxidation of toluene/$NO_x$/$SO_2$ without introducing $NH_3$ gas. This indicated there was $NH_3$ present in the background air in the chamber, and also indicated that the effects of $NH_3$ on secondary aerosol formation might be underestimated in this study. The background $NH_3$ was derived from the partitioning of the deposited ammonium sulfate and nitrate on the chamber wall when humid air was introduced (Liu et al., 2015b). Unfortunately, due to the lack of appropriate instruments, we were not able to measure the

exact concentration of $NH_3$ in the background air in the chamber. It was estimated to be around 8 ppb based on the amount of ammonium salt and the gas-aerosol equilibrium calculated using the AIM Aerosol Thermodynamics Model. With this in mind, the experiments carried out without introducing $NH_3$ gas were considered "$NH_3$-poor" experiments in this study, while experiments with the introduction of $NH_3$ gas were considered "$NH_3$-rich" experiments, in which the estimated concentrations of $NH_3$ were more than twice the $SO_2$ concentrations and the oxidation products of $SO_2$ and $NO_x$ were fully neutralized by $NH_3$, according to the chemical composition of aerosols measured by the AMS. The details of the acid-base balance in the aerosols are shown in Fig. S4 in the supporting information.

To further quantify the effect of $SO_2$ on secondary aerosol formation, different concentrations of $SO_2$ were introduced under $NH_3$-poor and $NH_3$-rich conditions. The details of the experimental conditions are shown in Table 2. In these experiments, the concentrations of toluene were reduced compared to the experiments in Table 1 to simulate secondary aerosol formation under experimental conditions closer to real ambient conditions, and monodisperse $Al_2O_3$ seed particles with mode diameter about 100 nm were introduced into the chamber. As shown in Figure 4, similar to the seed-free experiments, the presence of $SO_2$ and $NH_3$ clearly increased secondary aerosol formation in toluene/$NO_x$ photooxidation in the presence of $Al_2O_3$ seed aerosols. In the experiments carried out in the presence of $Al_2O_3$ seed aerosols, the decrease of $NH_4NO_3$ was less obvious

337 in the experiment carried out in the absence of $SO_2$ under $NH_3$-rich
338 conditions than in experiment ATN, as indicated in Fig.S5 in the supporting
339 information and Fig.3. This might also indicate that generation of $NH_4NO_3$
340 was dependent on the surface area concentration of the particles, which
341 decreased the partitioning of $NH_4NO_3$ back to the gas phase, as discussed
342 above concerning the effects of co-existing $(NH_4)_2SO_4$.

343 Under both $NH_3$-poor and $NH_3$-rich conditions, all the detected
344 chemical species in the generated aerosol, including sulfate, organic
345 aerosol, nitrate and ammonium, increased linearly with increasing $SO_2$
346 concentrations, as shown in Figure 5. The increase was more significant in
347 a $NH_3$-rich environment than under $NH_3$-poor conditions, indicating a
348 synergistic effect of $SO_2$ and $NH_3$ on aerosol generation. Among the four
349 chemical species, nitrate generation increased most significantly with
350 respect to $SO_2$ concentration under $NH_3$-rich conditions, followed by
351 ammonium and organic aerosol, while sulfate was the least sensitive
352 species. Under $NH_3$-poor conditions, the sensitivity of these species
353 followed a different sequence, in which sulfate > nitrate > organic aerosol >
354 ammonium. The different sequences under $NH_3$-rich and $NH_3$-poor
355 conditions indicated that the presence of $SO_2$ and $NH_3$ not only contributed
356 aerosol surface for partitioning, but also enhanced the heterogeneous
357 process for secondary aerosol formation.
358
359 Table 2. Initial experimental conditions for toluene/$NO_x$ photooxidation in the
360 presence of different concentrations of $SO_2$ and $Al_2O_3$ seed particles under $NH_3$-poor

and $NH_3$-rich conditions

| | **Toluene$_0$** | **NO$_0$** | **NO$_x$-NO** | **SO$_2$** | **Al$_2$O$_3$** | **NH$_3$*** | **RH** | **T** |
|---|---|---|---|---|---|---|---|---|
| | *ppb* | *ppb* | *ppb* | *ppb* | *particle/cm$^3$* | *ppb* | *%* | *K* |
| | 188 | 147 | 60 | 0 | 2400 | 0 | 50 | 303 |
| $NH_3$-poor | 200 | 126 | 51 | 52 | 3100 | 0 | 50 | 303 |
| | 188 | 130 | 58 | 105 | 2100 | 0 | 50 | 303 |
| | 197 | 142 | 46 | 0 | 3300 | 105 | 50 | 303 |
| $NH_3$-rich | 220 | 147 | 50 | 26 | 3300 | 105 | 50 | 303 |
| | 207 | 145 | 49 | 52 | 3200 | 105 | 50 | 303 |

*Calculated according to the amount of $NH_3$ introduced and the volume of the reactor.

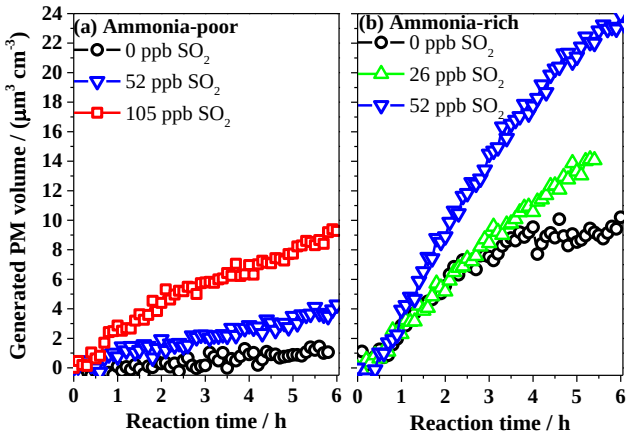


Figure 4. Secondary aerosol formation as a function of time with different concentrations of $SO_2$ in the photooxidation of toluene/$NO_x$ under $NH_3$-poor (a) and $NH_3$-rich (b) conditions. Experimental details are listed in Table 1.

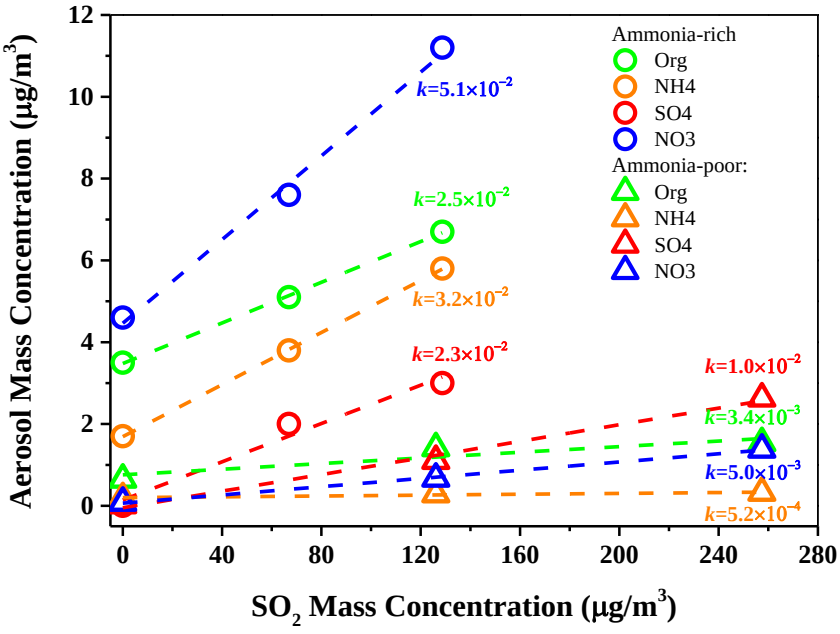


Figure 5. Formation of nitrate (blue), organic aerosol (green), sulfate (red), and ammonium salt (orange) as functions of $SO_2$ concentration in the photooxidation of toluene/$NO_x$ under $NH_3$-rich (circles) or $NH_3$-poor (triangles) conditions. The *k* values are the slopes of the fitted lines for each species. Experimental details are listed in Table 1.

Another synergetic effect we found in secondary inorganic aerosol formation was that sulfate formation was enhanced by the presence of $NH_3$. In both seed-free experiments and experiments in the presence of $Al_2O_3$ seed aerosols, the sulfate mass concentration was more than tripled under $NH_3$-rich conditions compared to an $NH_3$-poor environment. This is consistent with previous studies on the reactions of $SO_2$, $NO_2$ and $NH_3$ in smog chambers (Behera and Sharma, 2011) and the heterogeneous reaction between $NH_3$ and $SO_2$ on particle surfaces (Yang et al., 2016; Tursic et al.,

2004). According to the consumption of toluene, OH concentrations in the photooxidation experiments were estimated to range from 1.6 $\times 10^6$ molecules/cm$^3$ to 2.7 $\times 10^6$ molecules/cm$^3$. The reaction between these OH radicals and $SO_2$ contributed 35%-50% of the total $SO_2$ degradation in $NH_3$-poor experiments, while this ratio was reduced to 25%-30% in $NH_3$-rich experiments. This indicated that the heterogeneous process was an important pathway for inorganic aerosol formation in the photooxidation system, and the heterogeneous process was enhanced by the presence of $NH_3$. This result is consistent with the finding that failure to include the heterogeneous process in the model caused an underestimation of $SO_2$ decay in the chamber (Santiago et al., 2012). According to previous studies, $NH_3$ might provide surface Lewis basicity for $SO_2$ absorption on $Al_2O_3$ aerosols (Yang et al., 2016) and increase the amount of condensed water on the secondary aerosols (Tursic et al., 2004), and therefore enhance sulfate formation (Yang et al., 2016; Tursic et al., 2004).

**Secondary organic aerosol formation**

The presence of $NH_3$ and $SO_2$ caused significant formation of secondary inorganic aerosol, and also enhanced SOA formation. The increases of SOA mass in the presence of $NH_3$ and $SO_2$ are shown in Fig. 5. Similar trends for SOA yields can be found in the supporting information. In previous studies, Kleindienst et al. (2006) found that the presence of $SO_2$ did not disturb the dynamic reaction system of $\alpha$-pinene or isoprene in the presence of $NO_x$. In the present study, no obvious difference was found in

406 the OH concentration in experiments with different concentrations of $SO_2$
407 and $NH_3$. Therefore, it could be also speculated that the presence of $SO_2$
408 and $NH_3$ in this study did not significantly impact the gas phase oxidation
409 of hydrocarbons and mainly played a role in the aerosol phase.

410 The presence of $NH_3$ markedly increased aerosol formation in the
411 photooxidation of toluene/$NO_x$. In the seed-free toluene/$NO_x$
412 photooxidation experiments, the presence of $NH_3$ caused similar additional
413 amounts of organic aerosol mass and resulted in increases of 116% and 36%
414 in the absence or presence of $SO_2$, respectively. In the experiments carried
415 out in the presence of $Al_2O_3$ seed aerosols, the increase caused by $NH_3$ was
416 more significant, with the organic aerosol quantity increasing by a factor
417 of four to five. $NH_3$ may react with the oxycarboxylic acids from ring-
418 opening reactions in the photo-oxidation of toluene (Jang and Kamens,
419 2001), resulting in products with lower volatility. The presence of $NH_3$
420 might also change the surface properties of the aerosol and enhance
421 heterogeneous oxidation of organic products. As mentioned earlier in this
422 study, there was $NH_3$ present in the background air in the chamber, so the
423 effects of $NH_3$ on secondary aerosol formation might be underestimated in
424 this study. Detecting the concentration of $NH_3$ gas as a function of time and
425 quantifying the effects of $NH_3$ on secondary aerosol are meaningful, and
426 are expected to be studied in the future.

427 The enhancing effect of $NH_3$ on secondary aerosol formation in toluene
428 photooxidation was further attributed to its influence in heterogeneous
429 reactions. In the presence of $Al_2O_3$ seed particles, no obvious new particle

formation was detected in experiments without $SO_2$, as shown in Fig. 6(a) and Fig. 6(c). The presence of $NH_3$ caused a more noticeable growth in the size of the $Al_2O_3$ seed particles. The increase mainly took place after 0.5 hours of irradiation, and lasted for about an hour, with an average diameter growth of about 12 nm. In the two experiments carried out in the presence of 52 ppb $SO_2$ in Fig. 6(b) and Fig. 6(d), significant but similar new particle formation occurred. The maximum particle number concentrations detected by the SMPS were about 33000 particle/$cm^3$ and 34000 particle/$cm^3$ under $NH_3$-poor and $NH_3$-rich conditions, respectively. However, the growth of the seed aerosol in these two experiments was quite different. Under an $NH_3$-poor condition, the mode diameter of the seed aerosols grew from 100 nm to about 130 nm, while under an NH-rich condition it grew to about 220 nm. These results indicated that elevated $NH_3$ concentrations mainly affected secondary aerosol formation in the heterogeneous process.

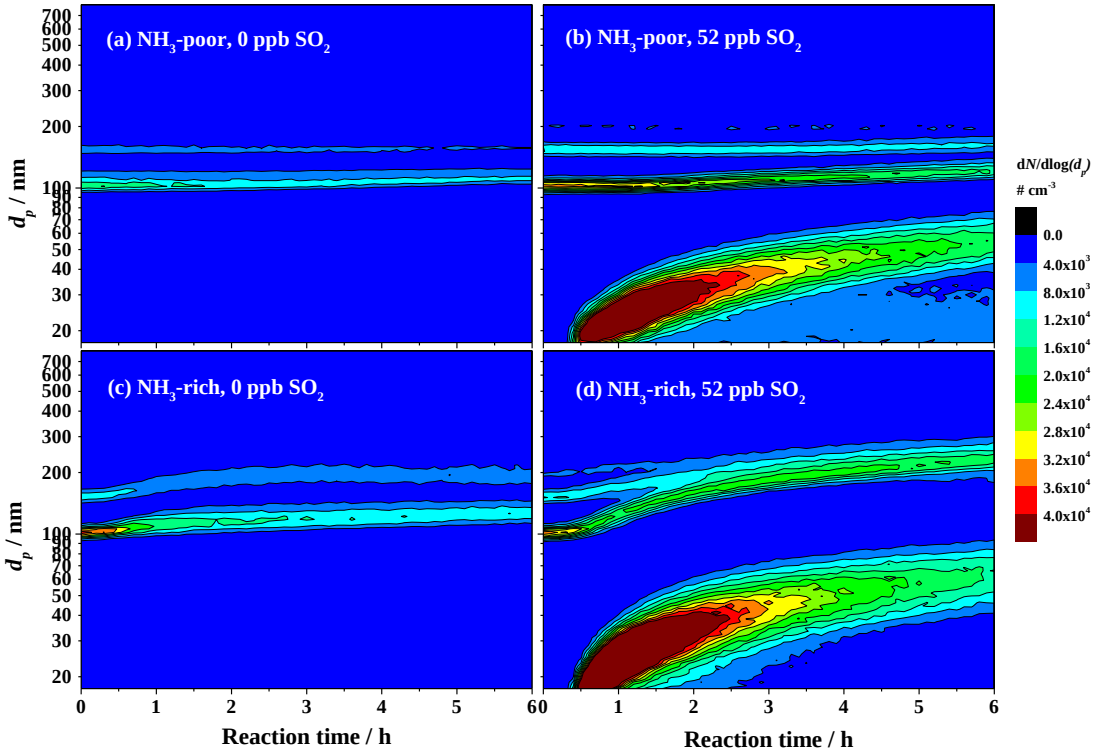


Figure 6. Size distributions of the suspended particles as a function of time during the reaction in photooxidation of toluene/$NO_x$ in the presence of $Al_2O_3$ seed particles. Experimental details are listed in Table 1.

The chemical properties of the SOA generated under different conditions of $NH_3$ and $SO_2$ were compared by applying PMF analysis to the AMS data. Two factors were identified from the analysis, with average elemental composition of $CH_{0.82}O_{0.75}N_{0.051}S_{0.0014}$ for Factor 1 and $CH_{1.05}O_{0.55}N_{0.039}S_{0.0017}$ for Factor 2. The difference mass spectra between the two factors are shown in Fig. 7. The abundance of $C_xH_y$ fragments was higher in Factor 2 than Factor 1, while oxygen and nitrogen contents in Factor 1 were higher than Factor 2. Meanwhile, as indicated in the red box in Fig. 7, fragments with high *m/z* were more abundant in Factor 2. Thus

we assigned Factor 1 to the highly oxidized organic component and some nitrogenous organic compounds, while Factor 2 was assigned to less-oxidized organic aerosol and some oligomers.

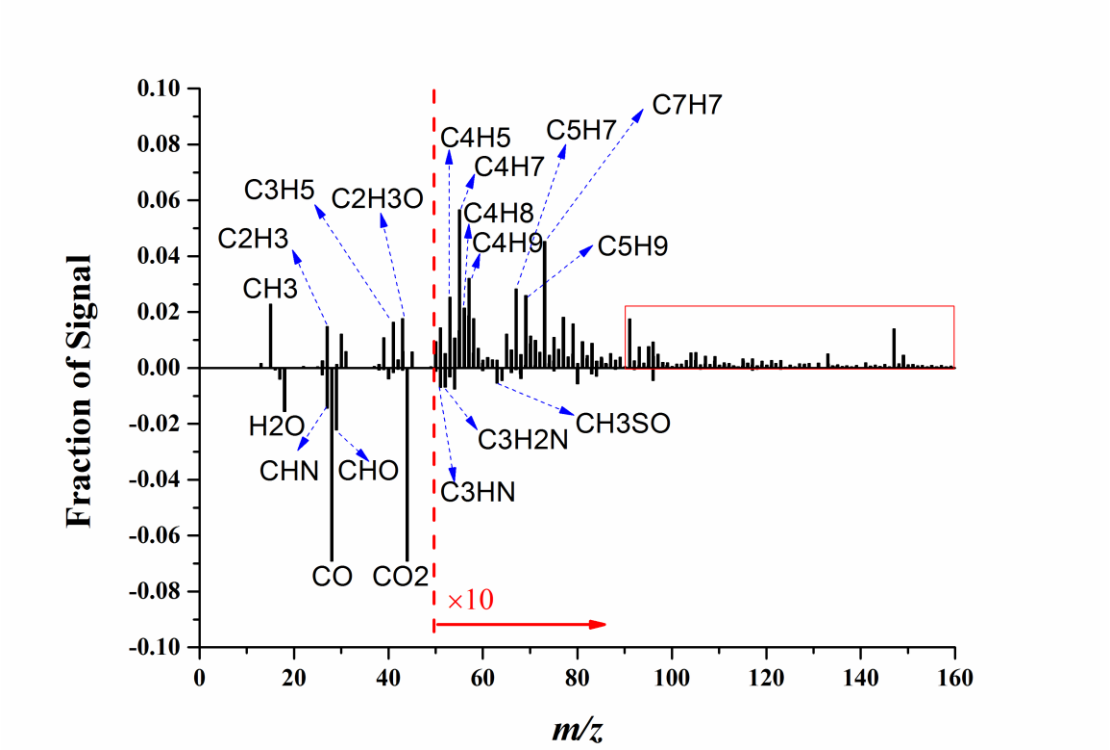


Figure 7. The difference mass spectra (Factor 2 – Factor 1) between the two factors of the generated organic aerosol identified by applying PMF analysis to the AMS data

These two factors had different temporal variations during the reaction. As indicated in Fig. 8, Factor 2 always increased at the beginning of the reaction but decreased after reaching a peak at 1 or 2 hours of irradiation. Factor 1 was generated later than Factor 2, while it continuously increased during the reaction. Comparing experiments with different concentrations of $SO_2$, the production of Factor 2 increased with increasing $SO_2$ under $NH_3$-poor conditions, while Factor 1 increased with increasing $SO_2$ under

an $NH_3$-rich environment. Similar results can also be found in Fig. 9. The higher production of Factor 2 with higher $SO_2$ under an $NH_3$-poor environment could be probably attributed to the well-known acid-catalysis effects of the oxidation product of $SO_2$, i.e. sulfuric acid, on heterogeneous aldol condensation (Offenberg et al., 2009; Jang et al., 2002; Gao et al., 2004). This is consistent with the fact that the aerosols in the $NH_3$-poor environment were quite acidic according to the simulation results of the AIM model, based on the chemical compositions of aerosols measured by the AMS. Under $NH_3$-rich conditions, however, Factor 1, which has higher contents of oxygen and nitrogen than Factor 2, dominated in the SOA formation. Meanwhile, the production of Factor 2 increased significantly with increasing $SO_2$ concentration in $NH_3$-rich conditions. This indicated that the formation of highly oxidized organic compounds and nitrogenous organic compounds was increased with higher concentrations of $SO_2$ under $NH_3$-rich conditions. By inference and from the results of AMS measurements, aerosol water increased as the initial concentration of $SO_2$ increased, since more inorganic aerosol was generated. Liggio and Li (2013) suggest that dissolution of primary polar gases into a partially aqueous aerosol contributes to the increase of organic mass and oxygen content on neutral and near-neutral seed aerosols, which would also take place in the $NH_3$-rich experiments and contribute to the generation of Factor 1.

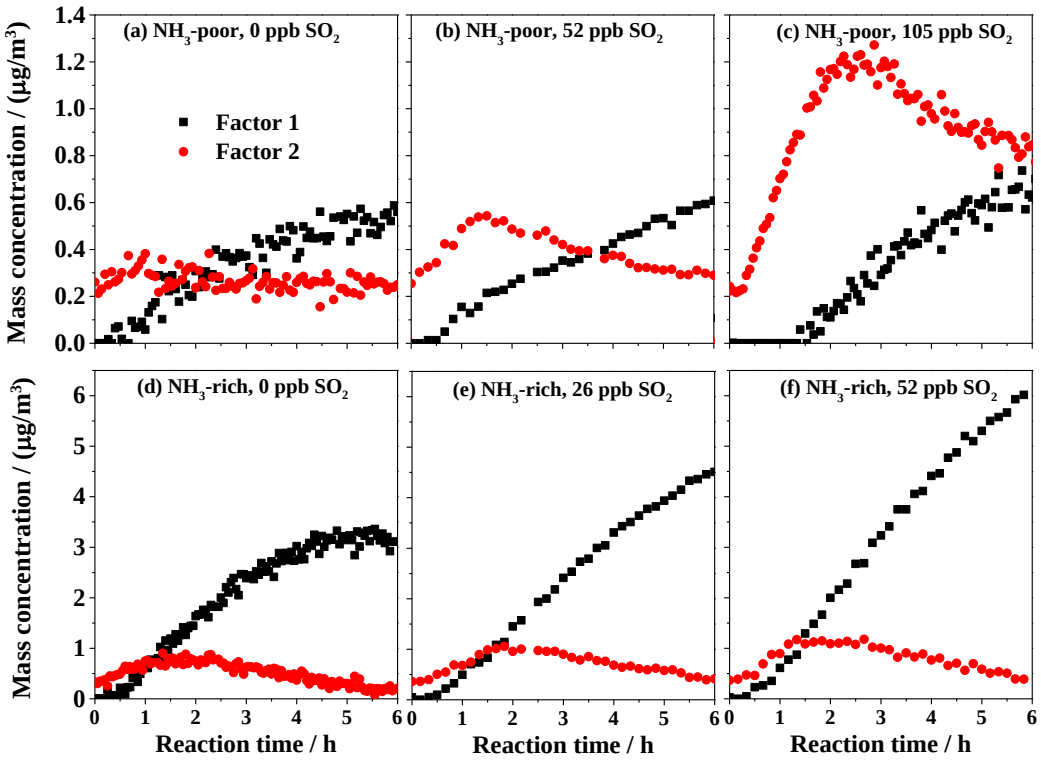


Figure 8. Temporal variations of Factor 1 and Factor 2 in the presence of different concentrations of $SO_2$ under $NH_3$-poor and $NH_3$-rich conditions.

Nitrogen-containing organics (NOC) are a potentially important aspect of SOA formation, and may have contributed to the increase of Factor 1 in this study. NOC might contain organonitrates, formed through reactions between organic peroxy radicals ($RO_2$) and NO (Arey et al., 2001), organic ammonium salts, generated in acid-base reactions between ammonia/ammonium and organic acid species (Liu et al., 2012b), and species with carbon covalently bonded to nitrogen, generated in reactions of ammonia/ammonium with carbonyl functional group organics (Wang et al., 2010). Although we were not able to measure NOC, some indirect estimation methods suggested by Farmer et al. (2010) could be applied. The details for estimation of the concentrations of organonitrates and NOC

with reduced N are given in the supporting information. Despite the uncertainty, there is an obvious increasing trend of organonitrates and NOC with reduced N with increasing $SO_2$ concentration under $NH_3$-rich conditions, as shown in Fig. 9. The increase ratio of NOC is higher than that of the organic aerosol or Factor 1 as $SO_2$ concentration increases. The estimated NOC contributed most of the increase in Factor 1 in $NH_3$-rich conditions. These results provide some evidence that the formation of organonitrates and NOC with reduced N (organic ammonium salts, imines, imidazole, and so on) played an important role in the increasing trend of SOA with $SO_2$ in an $NH_3$-rich environment. It was speculated that the higher surface acidity of aerosol formed in the presence of a high concentration of $SO_2$ favors NOC formation through $NH_3$ uptake by SOA, as observed in a recent work (Liu et al., 2015b).

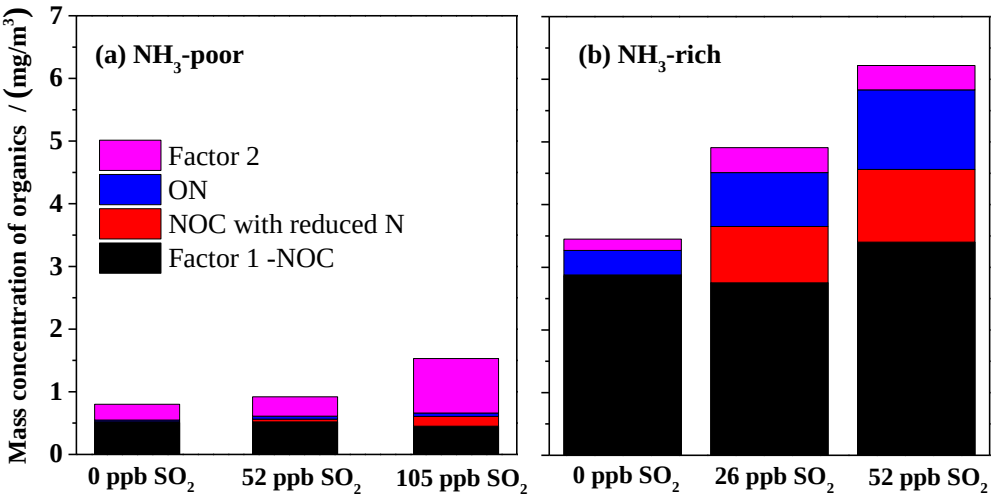


Figure 9. The estimated concentrations of NOC (ON+NOC with reduced N) and the two factors (identified by PMF analysis) in SOA as a function of $SO_2$ concentration in photooxidation of toluene/$NO_x$

under (a) $NH_3$-poor and (b) $NH_3$-rich conditions

## Conclusions

In the photooxidation system of toluene/$NO_x$, the presence of $SO_2$ and/or $NH_3$ increased secondary aerosol formation markedly, regardless of whether $Al_2O_3$ seed aerosol was present or not. Some synergetic effects in the heterogeneous process were observed in secondary inorganic aerosol formation in addition to the generation of ammonium and sulfate from $NH_3$ and $SO_2$. Specifically, the generation of $NH_4NO_3$ was found to be highly dependent on the surface area concentration of suspended particles, and was enhanced by increased $SO_2$ concentration. Meanwhile, sulfate formation was also increased in the presence of $NH_3$. The absorbed $NH_3$ might provide liquid surface layers for the absorption and subsequent reaction for $SO_2$ and organic products, and therefore, enhance sulfate and SOA formation. $NH_3$ mainly influenced secondary aerosol formation in the heterogeneous process, resulting in significant growth of seed aerosols, but had little influence on new particle generation. In the experiments carried out in the presence of $Al_2O_3$ seed aerosols, sulfate, organic aerosol, nitrate and ammonium were all found to increase linearly with increasing $SO_2$ concentration in toluene/$NO_x$ photooxidation. The increase of these four species was more obvious under $NH_3$-rich conditions, and the order of their sensitivity was different from that under $NH_3$-poor conditions. The better correlation between secondary aerosol formation and particle surface area than that with particle volume indicated an enhancement effect in the

heterogeneous process rather than in bulk reactions.

Two factors were identified in the PMF analysis of the AMS data. One factor assigned to less-oxidized organic aerosol and some oligomers increased with increasing $SO_2$ under $NH_3$-poor conditions, mainly due to the well-known acid catalytic effects of the acid products on SOA formation in the heterogeneous process. The other factor, assigned to the highly oxidized organic component and some nitrogenous organic compounds, increased with increasing $SO_2$ under an $NH_3$-rich environment, with NOC (organonitrates and NOC with reduced N) contributing most of the increase.

This study indicated that the synergistic effects between inorganic pollutants could substantially enhance secondary inorganic aerosol formation. Meanwhile, the presence of inorganic gas pollutants, i.e. $SO_2$ and $NH_3$, promoted SOA formation markedly. Synergistic formation of secondary inorganic and organic aerosol might increase the secondary aerosol load in the atmosphere. These synergistic effects were related to the heterogeneous process on the aerosol surface, and need to be quantified and considered in air quality models.

## Acknowledgments

This work was supported by the National Natural Science Foundation of China (21407158), the “Strategic Priority Research Program” of the Chinese Academy of Sciences (XDB05010300, XDB05040100, XDB05010102), and the special fund of the State Key Joint Laboratory of

Environment Simulation and Pollution Control (14Z04ESPCR). This work was also financially and technically supported by Toyota Motor Corporation and Toyota Central Research and Development Laboratories Inc.

## References

Amarnath, V., Anthony, D. C., Amarnath, K., Valentine, W. M., Wetterau, L. A., and Graham, D. G.: Intermediates in the Paal-Knorr Synthesis of Pyrroles, J. Org. Chem., 56, 6924-6931, doi:10.1021/jo00024a040, 1991.

Arey, J., Aschmann, S. M., Kwok, E. S. C., and Atkinson, R.: Alkyl nitrate, hydroxyalkyl nitrate, and hydroxycarbonyl formation from the NOx-air photooxidations of C-5-C-8 n-alkanes, J. Phys. Chem. A, 105, 1020-1027, doi:10.1021/jp003292z, 2001.

Bai, Y., Thompson, G. E., and Martinez-Ramirez, S.: Effects of $NO_2$ on oxidation mechanisms of atmospheric pollutant $SO_2$ over Baumberger sandstone, Build. Environ., 41, 486-491, doi:10.1016/j.buildenv.2005.02.007, 2006.

Bauduin, S., Clarisse, L., Hadji-Lazaro, J., Theys, N., Clerbaux, C., and Coheur, P. F.: Retrieval of near-surface sulfur dioxide ($SO_2$) concentrations at a global scale using IASI satellite observations, Atmos. Meas. Tech., 9, 721-740, doi:10.5194/amt-9-721-2016, 2016.

Behera, S. N., and Sharma, M.: Degradation of $SO_2$, $NO_2$ and $NH_3$ leading to formation of secondary inorganic aerosols: An environmental chamber study, Atmos. Environ., 45, 4015-4024, doi:10.1016/j.atmosenv.2011.04.056, 2011.

Carslaw, K. S., Clegg, S. L., and Brimblecombe, P.: A thermodynamic model of the system HCl-$HNO_3$-$H_2SO_4$-$H_2O$, including solubilities of HBr, from less-than-200 to 328 K, J. Phys. Chem., 99, 11557-11574, doi:10.1021/j100029a039, 1995.

Chu, B., Hao, J., Takekawa, H., Li, J., Wang, K., and Jiang, J.: The remarkable effect of $FeSO_4$ seed aerosols on secondary organic aerosol formation from photooxidation of α-pinene/NOx and toluene/NOx, Atmos. Environ., 55, 26-34, doi:10.1016/j.atmosenv.2012.03.006, 2012.

Chu, B., Liu, Y., Li, J., Takekawa, H., Liggio, J., Li, S.-M., Jiang, J., Hao, J., and He, H.: Decreasing effect and mechanism of $FeSO_4$ seed particles on secondary organic aerosol in α-pinene photooxidation, Environ. Pollut., 193, 88-93, doi:10.1016/j.envpol.2014.06.018, 2014.

Clegg, S. L., Brimblecombe, P., and Wexler, A. S.: Thermodynamic model of the system $H^+$-$NH_4^+$-$SO_4^{2-}$-$NO_3^-$-$H_2O$ at tropospheric temperatures, J. Phys. Chem. A, 102, 2137-2154, doi:10.1021/jp973042r, 1998.

605 Clegg, S. L., and Brimblecombe, P.: Comment on the "Thermodynamic dissociation constant of the
606 bisulfate ion from Raman and ion interaction modeling studies of aqueous sulfuric acid at low
607 temperatures", J. Phys. Chem. A, 109, 2703-2706, doi:10.1021/jp0401170, 2005.
608 Dan, M., Zhuang, G., Li, X., Tao, H., and Zhuang, Y.: The characteristics of carbonaceous species and
609 their sources in $PM_{2.5}$ in Beijing, Atmos. Environ., 38, 3443-3452, doi:10.1016/j.atmosenv.2004.02.052,
610 2004.
611 Dong, W. X., Xing, J., and Wang, S. X.: Temporal and spatial distribution of anthropogenic ammonia
612 emissions in China: 1994–2006, Huanjingkexue, 31, 1457-1463, doi: 10.13227/j.hjkx.2010.07.008, 2010.
613 Duan, F., He, K., Ma, Y., Jia, Y., Yang, F., Lei, Y., Tanaka, S., and Okuta, T.: Characteristics of
614 carbonaceous aerosols in Beijing, China, Chemosphere, 60, 355-364,
615 doi:10.1016/j.chemosphere.2004.12.035, 2005.
616 Edney, E. O., Kleindienst, T. E., Jaoui, M., Lewandowski, M., Offenberg, J. H., Wang, W., and Claeys,
617 M.: Formation of 2-methyl tetrols and 2-methylglyceric acid in secondary organic aerosol from
618 laboratory irradiated isoprene/$NO_X$/$SO_2$/air mixtures and their detection in ambient $PM_{2.5}$ samples
619 collected in the eastern United States, Atmos. Environ., 39, 5281-5289,
620 doi:10.1016/j.atmosenv.2005.05.031, 2005.
621 Farmer, D. K., Matsunaga, A., Docherty, K. S., Surratt, J. D., Seinfeld, J. H., Ziemann, P. J., and Jimenez,
622 J. L.: Response of an aerosol mass spectrometer to organonitrates and organosulfates and implications
623 for atmospheric chemistry, Proc. Natl. Acad. Sci. USA, 107, 6670-6675, doi:10.1073/pnas.0912340107,
624 2010.
625 Fu, X., Wang, S. X., Ran, L. M., Pleim, J. E., Cooter, E., Bash, J. O., Benson, V., and Hao, J. M.:
626 Estimating $NH_3$ emissions from agricultural fertilizer application in China using the bi-directional
627 CMAQ model coupled to an agro-ecosystem model, Atmos. Chem. Phys., 15, 6637-6649,
628 doi:10.5194/acp-15-6637-2015, 2015.
629 Gao, S., Ng, N. L., Keywood, M., Varutbangkul, V., Bahreini, R., Nenes, A., He, J. W., Yoo, K. Y.,
630 Beauchamp, J. L., Hodyss, R. P., Flagan, R. C., and Seinfeld, J. H.: Particle phase acidity and oligomer
631 formation in secondary organic aerosol, Environ. Sci. & Technol., 38, 6582-6589,
632 doi:10.1021/es049125k, 2004.
633 Hallquist, M., Stewart, D. J., Stephenson, S. K., and Cox, R. A.: Hydrolysis of $N_2O_5$ on sub-micron
634 sulfate aerosols, Phys. Chem. Chem. Phys., 5, 3453-3463, doi:10.1039/b301827j, 2003.
635 He, H., Wang, Y., Ma, Q., Ma, J., Chu, B., Ji, D., Tang, G., Liu, C., Zhang, H., and Hao, J.: Mineral dust
636 and NOx promote the conversion of $SO_2$ to sulfate in heavy pollution days, Sci. Rep., 4, 04172,
637 doi:10.1038/srep04172, 2014.
638 Hu, J. H., and Abbatt, J. P. D.: Reaction probabilities for $N_2O_5$ hydrolysis on sulfuric acid and ammonium
639 sulfate aerosols at room temperature, J. Phys. Chem. A, 101, 871-878, doi:10.1021/jp9627436, 1997.
640 Jang, M. S., and Kamens, R. M.: Characterization of secondary aerosol from the photooxidation of

641 toluene in the presence of NOx and 1-propene, Environ. Sci. & Technol., 35, 3626-3639,
642 doi:10.1021/es010676+, 2001.
643 Jang, M. S., Czoschke, N. M., Lee, S., and Kamens, R. M.: Heterogeneous atmospheric aerosol
644 production by acid-catalyzed particle-phase reactions, Science, 298, 814-817,
645 doi:10.1126/science.1075798, 2002.
646 Jaoui, M., Edney, E. O., Kleindienst, T. E., Lewandowski, M., Offenberg, J. H., Surratt, J. D., and
647 Seinfeld, J. H.: Formation of secondary organic aerosol from irradiated alpha-pinene/toluene/NOx
648 mixtures and the effect of isoprene and sulfur dioxide, J. Geophys. Res.- Atmos., 113, D09303,
649 doi:10.1029/2007jd009426, 2008.
650 Kleindienst, T. E., Edney, E. O., Lewandowski, M., Offenberg, J. H., and Jaoui, M.: Secondary organic
651 carbon and aerosol yields from the irradiations of isoprene and alpha-pinene in the presence of NOx and
652 $SO_2$, Environ. Sci. & Technol., 40, 3807-3812, doi:10.1021/es052446r, 2006.
653 Li, C., Marufu, L. T., Dickerson, R. R., Li, Z., Wen, T., Wang, Y., Wang, P., Chen, H., and Stehr, J. W.:
654 In situ measurements of trace gases and aerosol optical properties at a rural site in northern China during
655 East Asian Study of Tropospheric Aerosols: An International Regional Experiment 2005, J. Geophys.
656 Res.- Atmos., 112, D22S04, doi:10.1029/2006JD007592, 2007.
657 Li, W. J., Shao, L. Y., Shi, Z. B., Chen, J. M., Yang, L. X., Yuan, Q., Yan, C., Zhang, X. Y., Wang, Y. Q.,
658 Sun, J. Y., Zhang, Y. M., Shen, X. J., Wang, Z. F., and Wang, W. X.: Mixing state and hygroscopicity of
659 dust and haze particles before leaving Asian continent, J. Geophys. Res.- Atmos., 119, 1044-1059,
660 doi:10.1002/2013jd021003, 2014.
661 Liggio, J., and Li, S. M.: Reactive uptake of pinonaldehyde on acidic aerosols, J. Geophys. Res.- Atmos.,
662 111, D24303, doi:10.1029/2005jd006978, 2006.
663 Liggio, J., Li, S. M., Brook, J. R., and Mihele, C.: Direct polymerization of isoprene and alpha-pinene
664 on acidic aerosols, Geophys. Res. Lett., 34, doi:10.1029/2006gl028468, 2007.
665 Liggio, J., and Li, S. M.: Reversible and irreversible processing of biogenic olefins on acidic aerosols,
666 Atmos. Chem. Phys., 8, 2039-2055, doi:10.5194/acp-8-2039-2008 2008.
667 Liggio, J., and Li, S. M.: A new source of oxygenated organic aerosol and oligomers, Atmos. Chem.
668 Phys., 13, 2989-3002, doi:10.5194/acp-13-2989-2013, 2013.
669 Lin, Y. H., Knipping, E. M., Edgerton, E. S., Shaw, S. L., and Surratt, J. D.: Investigating the influences
670 of $SO_2$ and $NH_3$ levels on isoprene-derived secondary organic aerosol formation using conditional
671 sampling approaches, Atmos. Chem. Phys., 13, 8457-8470, doi:10.5194/acp-13-8457-2013, 2013.
672 Liu, C., Liu, Y., Ma, Q., and He, H.: Mesoporous transition alumina with uniform pore structure
673 synthesized by alumisol spray pyrolysis, Chem. Eng. J., 163, 133-142, doi: 10.1016/j.cej.2010.07.046,
674 2010.
675 Liu, C., Ma, Q., Liu, Y., Ma, J., and He, H.: Synergistic reaction between $SO_2$ and $NO_2$ on mineral oxides:
676 a potential formation pathway of sulfate aerosol, Phys. Chem. Chem. Phys., 14, 1668-1676,

677 doi:10.1039/c1cp22217a, 2012a.
678 Liu, X. G., Li, J., Qu, Y., Han, T., Hou, L., Gu, J., Chen, C., Yang, Y., Liu, X., Yang, T., Zhang, Y., Tian,
679 H., and Hu, M.: Formation and evolution mechanism of regional haze: a case study in the megacity
680 Beijing, China, Atmos. Chem. Phys., 13, 4501-4514, doi:10.5194/acp-13-4501-2013, 2013.
681 Liu, X. G., Sun, K., Qu, Y., Hu, M., Sun, Y. L., Zhang, F., and Zhang, Y. H.: Secondary Formation of
682 Sulfate and Nitrate during a Haze Episode in Megacity Beijing, China, Aerosol Air Qual. Res., 15, 2246-
683 2257, doi:10.4209/aaqr.2014.12.0321, 2015a.
684 Liu, Y., Ma, Q., and He, H.: Heterogeneous Uptake of Amines by Citric Acid and Humic Acid, Environ.
685 Sci. & Technol., 46, doi:11112-11118, 10.1021/es302414v, 2012b.
686 Liu, Y., Liggio, J., Staebler, R., and Li, S. M.: Reactive uptake of ammonia to secondary organic aerosols:
687 kinetics of organonitrogen formation, Atmos. Chem. Phys., 15, 13569-13584, doi:10.5194/acp-15-
688 13569-2015, 2015b.
689 Lu, Z., Streets, D. G., Zhang, Q., Wang, S., Carmichael, G. R., Cheng, Y. F., Wei, C., Chin, M., Diehl, T.,
690 and Tan, Q.: Sulfur dioxide emissions in China and sulfur trends in East Asia since 2000, Atmos. Chem.
691 Phys., doi:10, 6311-6331, 10.5194/acp-10-6311-2010, 2010.
692 Meng, Z., Xie, Y., Jia, S., Zhang, R., Lin, W., Xu, X., and Yang, W.: Characteristics of Atmospheric
693 Ammonia at Gucheng, a Rural Site on North China Plain in Summer of 2013, J. Appl. Meteor. Sci., 26,
694 141-150, doi:10.11898/1001-7313.20150202, 2015.
695 Meyer, N. K., Duplissy, J., Gysel, M., Metzger, A., Dommen, J., Weingartner, E., Alfarra, M. R., Prevot,
696 A. S. H., Fletcher, C., Good, N., McFiggans, G., Jonsson, A. M., Hallquist, M., Baltensperger, U., and
697 Ristovski, Z. D.: Analysis of the hygroscopic and volatile properties of ammonium sulphate seeded and
698 unseeded SOA particles, Atmos. Chem. Phys., 9, 721-732, doi: 10.5194/acp-9-721-2009, 2009.
699 Na, K., Song, C., and Cocker, D. R.: Formation of secondary organic aerosol from the reaction of styrene
700 with ozone in the presence and absence of ammonia and water, Atmos. Environ., 40, 1889-1900,
701 doi:10.1016/j.atmosenv.2005.10.063, 2006.
702 Na, K., Song, C., Switzer, C., and Cocker, D. R.: Effect of ammonia on secondary organic aerosol
703 formation from alpha-Pinene ozonolysis in dry and humid conditions, Environ. Sci. & Technol., 41,
704 6096-6102, doi:10.1021/es061956y, 2007.
705 Ng, N. L., Herndon, S. C., Trimborn, A., Canagaratna, M. R., Croteau, P. L., Onasch, T. B., Sueper, D.,
706 Worsnop, D. R., Zhang, Q., Sun, Y. L., and Jayne, J. T.: An Aerosol Chemical Speciation Monitor (ACSM)
707 for routine monitoring of the composition and mass concentrations of ambient aerosol, Aerosol Sci.
708 Technol., 45, 770-784, doi:10.1080/02786826.2011.560211, 2011.
709 Offenberg, J. H., Lewandowski, M., Edney, E. O., Kleindienst, T. E., and Jaoui, M.: Influence of Aerosol
710 Acidity on the Formation of Secondary Organic Aerosol from Biogenic Precursor Hydrocarbons,
711 Environ. Sci. & Technol., 43, 7742-7747, doi:10.1021/es901538e, 2009.
712 Pathak, R. K., Wu, W. S., and Wang, T.: Summertime PM2.5 ionic species in four major cities of China:

713 nitrate formation in an ammonia-deficient atmosphere, Atmos. Chem. Phys., 9, 1711-1722, doi:
714 10.5194/acp-9-1711-2009, 2009.
715 Santiago, M., Garcia Vivanco, M., and Stein, A. F.: $SO_2$ effect on secondary organic aerosol from a
716 mixture of anthropogenic VOCs: experimental and modelled results, Int. J. Environ. Pollut., 50, 224-233,
717 doi:10.1504/IJEP.2012.051195, 2012.
718 Schmitt-Kopplin, P., Gelencser, A., Dabek-Zlotorzynska, E., Kiss, G., Hertkorn, N., Harir, M., Hong, Y.,
719 and Gebefuegi, I.: Analysis of the Unresolved Organic Fraction in Atmospheric Aerosols with Ultrahigh-
720 Resolution Mass Spectrometry and Nuclear Magnetic Resonance Spectroscopy: Organosulfates As
721 Photochemical Smog Constituents, Anal. Chem., 82, 8017-8026, doi:10.1021/ac101444r, 2010.
722 Sun, Y., Wang, Y. S., and Zhang, C. C.: Measurement of the vertical profile of atmospheric $SO_2$ during
723 the heating period in Beijing on days of high air pollution, Atmos. Environ., 43, 468-472,
724 doi:10.1016/j.atmosenv.2008.09.057, 2009.
725 Takekawa, H., Minoura, H., and Yamazaki, S.: Temperature dependence of secondary organic aerosol
726 formation by photo-oxidation of hydrocarbons, Atmos. Environ., 37, 3413-3424, doi:10.1016/s1352-
727 2310(03)00359-5, 2003.
728 Tursic, J., and Grgic, I.: Influence of $NO_2$ on S(IV) oxidation in aqueous suspensions of aerosol particles
729 from two different origins, Atmos. Environ., 35, 3897-3904, doi:10.1016/s1352-2310(01)00142-x, 2001.
730 Tursic, J., Berner, A., Podkrajsek, B., and Grgic, I.: Influence of ammonia on sulfate formation under
731 haze conditions, Atmos. Environ., 38, 2789-2795, doi:10.1016/j.atmosenv.2004.02.036, 2004.
732 Updyke, K. M., Nguyen, T. B., and Nizkorodov, S. A.: Formation of brown carbon via reactions of
733 ammonia with secondary organic aerosols from biogenic and anthropogenic precursors, Atmos. Environ.,
734 63, 22-31, doi:10.1016/j.atmosenv.2012.09.012, 2012.
735 Wang, L., Wen, L., Xu, C., Chen, J., Wang, X., Yang, L., Wang, W., Yang, X., Sui, X., Yao, L., and Zhang,
736 Q.: HONO and its potential source particulate nitrite at an urban site in North China during the cold
737 season, Sci. Total Environ., 538, 93-101, doi:10.1016/j.scitotenv.2015.08.032, 2015a.
738 Wang, S. W., Zhang, Q., Martin, R. V., Philip, S., Liu, F., Li, M., Jiang, X. J., and He, K. B.: Satellite
739 measurements oversee China's sulfur dioxide emission reductions from coal-fired power plants, Environ.
740 Res. Lett., 10, 9, doi:10.1088/1748-9326/10/11/114015, 2015b.
741 Wang, X. F., Gao, S., Yang, X., Chen, H., Chen, J. M., Zhuang, G. S., Surratt, J. D., Chan, M. N., and
742 Seinfeld, J. H.: Evidence for High Molecular Weight Nitrogen-Containing Organic Salts in Urban
743 Aerosols, Environ. Sci. & Technol., 44, 4441-4446, doi:10.1021/es1001117, 2010.
744 Wang, Z., Wang, T., Guo, J., Gao, R., Xue, L. K., Zhang, J. M., Zhou, Y., Zhou, X. H., Zhang, Q. Z., and
745 Wang, W. X.: Formation of secondary organic carbon and cloud impact on carbonaceous aerosols at
746 Mount Tai, North China, Atmos. Environ., 46, 516-527, doi:10.1016/j.atmosenv.2011.08.019, 2012.
747 Wen, L. A., Chen, J. M., Yang, L. X., Wang, X. F., Xu, C. H., Sui, X. A., Yao, L., Zhu, Y. H., Zhang, J.
748 M., Zhu, T., and Wang, W. X.: Enhanced formation of fine particulate nitrate at a rural site on the North

China Plain in summer: The important roles of ammonia and ozone, Atmos. Environ., 101, 294-302, doi:10.1016/j.atmosenv.2014.11.037, 2015.

Wu, S., Lu, Z. F., Hao, J. M., Zhao, Z., Li, J. H., Hideto, T., Hiroaki, M., and Akio, Y.: Construction and characterization of an atmospheric simulation smog chamber, Adv. Meteorol., 24, 250-258, doi:10.1007/s00376-007-0250-3, 2007.

Yang, F., Tan, J., Zhao, Q., Du, Z., He, K., Ma, Y., Duan, F., Chen, G., and Zhao, Q.: Characteristics of PM2.5 speciation in representative megacities and across China, Atmos. Chem. Phys., 11, 5207-5219, doi:10.5194/acp-11-5207-2011, 2011.

Yang, W., He, H., Ma, Q., Ma, J., Liu, Y., Liu, P., and Mu, Y.: Synergistic formation of sulfate and ammonium resulting from reaction between $SO_2$ and $NH_3$ on typical mineral dust, Phys. Chem. Chem. Phys., 18, 956-964, doi:10.1039/c5cp06144j, 2016.

Ye, X. N., Ma, Z., Zhang, J. C., Du, H. H., Chen, J. M., Chen, H., Yang, X., Gao, W., and Geng, F. H.: Important role of ammonia on haze formation in Shanghai, Environ. Res. Lett., 6, 024019, doi:10.1088/1748-9326/6/2/024019, 2011.

Zhang, Q., Shen, Z. X., Cao, J. J., Zhang, R. J., Zhang, L. M., Huang, R. J., Zheng, C. J., Wang, L. Q., Liu, S. X., Xu, H. M., Zheng, C. L., and Liu, P. P.: Variations in $PM_{2.5}$, TSP, BC, and trace gases ($NO_2$, $SO_2$, and $O_3$) between haze and non-haze episodes in winter over Xi'an, China, Atmos. Environ., 112, 64-71, doi:10.1016/j.atmosenv.2015.04.033, 2015.

Zhao, P. S., Dong, F., He, D., Zhao, X. J., Zhang, X. L., Zhang, W. Z., Yao, Q., and Liu, H. Y.: Characteristics of concentrations and chemical compositions for PM2.5 in the region of Beijing, Tianjin, and Hebei, China, Atmos. Chem. Phys., 13, 4631-4644, doi:10.5194/acp-13-4631-2013, 2013.

Zou, Y., Deng, X. J., Zhu, D., Gong, D. C., Wang, H., Li, F., Tan, H. B., Deng, T., Mai, B. R., Liu, X. T., and Wang, B. G.: Characteristics of 1 year of observational data of VOCs, NOx and $O_3$ at a suburban site in Guangzhou, China, Atmos. Chem. Phys., 15, 6625-6636, doi:10.5194/acp-15-6625-2015, 2015.